Journal of Petroleum Science and Engineering 126 (2015) 201–210

Contents lists available at ScienceDirect

Journal of Petroleum Science and Engineering

journal homepage: www.elsevier.com/locate/petrol

Deep bed and cake filtration of two-size particle suspension in porous media

Rebeca N. Sacramento [a], Yulong Yang [b], Zhenjiang You [b,*], Alex Waldmann [c], André L. Martins [c], Alexandre S.L. Vaz [a], Pacelli L.J. Zitha [d], Pavel Bedrikovetsky [b]

[a] Laboratory of Exploration and Production Engineering LENEP, North Fluminense State University UENF, Macaé, RJ, Brazil
[b] Australian School of Petroleum, The University of Adelaide, SA 5005, Australia
[c] Research and Development Centre CENPES, Petrobras, Rio de janeiro, RJ, Brazil
[d] Department of Geotechnology, Delft University of Technology, Delft, The Netherlands

ARTICLE INFO

Article history:
Received 11 September 2013
Accepted 4 December 2014
Available online 13 December 2014

Keywords:
External cake
Deep bed filtration
Cake formation
Transition time
Porous media
Analytical solution

ABSTRACT

Formation of low permeable external filter cake during drilling and water injection has been widely reported in the literature. It may cause significant decrease in well index. The process is very sensitive to size distribution of injected particles. We propose a new mathematical model for cake formation with deep bed filtration for two-particle-size injection. The basic equations account for three stages: formation of cake from large particles with simultaneous deep bed filtration of small particles; small particle capture in the cake with formation of the internal cake inside the external cake; build-up of the uniform cake from the mixture of two-size particles. The analytical model is derived for three stages. Two regimes of the cake formation are identified, which correspond to the high and low concentrations of injected small particles. The laboratory coreflood with two-particle-size suspension injection with monitoring the rate and pressure drop along the core is performed. The matched mathematical model shows good agreement with the laboratory data.

1. Introduction

Deep bed filtration and external filter cake formation are common phenomena encountered in the petroleum industry, which may lead to severe permeability decline and formation damage (Ghalambor and Economides, 2002; Ding et al., 2004; Ding and Renard, 2005; Ding et al., 2006; Wagner et al., 2006; Civan, 2007; Dalmazzone et al., 2007; Quintero et al., 2007; Ding et al., 2008; Salimi et al., 2009; Lohne et al., 2010; Karimi et al., 2011). During drilling, completion or produced water reinjection, fluids carrying suspended particles enter the wellbore. Due to the pressure difference between the wellbore and the reservoir formation (the pressure in the well is higher than that of the formation during the overbalanced drilling), the fluid penetrates into the formation. Particles suspended in the fluid with sizes larger than the pore throats in the formation may accumulate on the wellbore surface, forming a cake. This process is known as the external cake formation (Ruth, 1935; Ochi et al., 1999; Parn-anurak and Engler, 2005; Ochi et al., 2007; Windarto et al., 2011; Ytrehus et al., 2013). However, those fine particles smaller than the pore throats of external cake may pass through the cake and penetrate into the formation. During the filtration, the solid particles suspended in the carrier fluid may be separated from the liquid phase due to several different mechanisms, such as gravity, Brownian motion, size exclusion, etc. (Ochi and Vernoux, 1999; Shapiro et al., 2007; Yuan and Shapiro, 2011; You et al., 2013; Yuan et al., 2013). The process of suspension transport in porous media accompanied by particle capture in the pores is called deep bed filtration (Payatakes et al., 1974; Pang and Sharma, 1997; Khilar and Fogler, 1998; Bedrikovetsky, 2008; You et al., 2014).

The classical deep bed filtration (DBF) model developed by Herzig et al. (1970) consists of two equations—one for particle population balance and the other for particle capture kinetics. The macro scale functions including suspended and retained particle concentrations and the filtration coefficient as a function of retained concentration are introduced into the model. Analytical solutions to the direct problems for model prediction (Herzig et al., 1970) and to the inverse problems for parameter determination (Wennberg and Sharma, 1997; Bedrikovetsky et al., 2001) have been obtained. This model has shown a good agreement with experimental data and has been used to predict the well injectivity decline based on the experimental core flood data.

* Corresponding author. Fax: +61 8 8303 4345.
E-mail address: zyou@asp.adelaide.edu.au (Z. You).

http://dx.doi.org/10.1016/j.petrol.2014.12.001
0920-4105/

Nomenclature

L	core length, m
r_s	small particle radius, m
r_l	large particle radius, m
c_1^0	initial total particle concentration, ppm
c_2^0	initial large particle concentration, ppm
c_3^0	initial small particle concentration, ppm
D_p	particle diameter, m
D_3	speed of mixture cake growth
J	impedance
$k_m(0)$	initial core permeability, m^2
k_{ec12}	permeability of external cake filled by internal cake of small particles, m^2
R	ratio of external cake porosity and core porosity
ΔP_{ec1}	pressure drop between the fronts of external and internal cake, Pa
ΔP_{ec2}	pressure drop between the front of internal cake and the core inlet, Pa
ΔP_m	pressure drop of the core, Pa
S	dimensionless retention concentration
U	Darcy velocity, m/s
T	dimensionless time
t	time, s
T_{tr}	transition time
T_3	catching-up time of the internal cake front
X	dimensionless coordinate
x	coordinate, m
z	internal cake thickness, m

Greek letters

α	critical coefficient
β	formation damage coefficient
λ	filtration coefficient
μ	viscosity of suspension, Pa s
τ	tortuosity
ϕ_1	core porosity
ϕ_2	porosity of internal cake
ϕ_3	porosity of external cake
ϕ_4	porosity of the mixture cake
σ	retained particle concentration, m^{-3}

Subscripts

m	medium
c	cake
ec	external cake
ecmix	mixture cake

Analytical models for deep bed filtration with constant and varying rates for linear and axisymmetric flows have been derived by Civan and Rasmussen (2005). Numerous laboratory tests have been treated by the analytical model with the observation of good agreement between the analytical and experimental modelling. More complex model for deep bed filtration is proposed by Civan and Nguyen (2005). All pathways are divided into two parts—those plugging and non-plugging. The analytical models as well as their tuning by laboratory tests have been performed.

During particle deep bed filtration through porous media, there exists a critical moment when the retention concentration of particles at the core inlet reaches its critical value (Khatib, 1994). After the moment, few particles can penetrate into the core. Instead, the new-coming particles form external cake only. This critical moment is termed as the transition time. The existence of transition time has been observed and its evaluation has been studied intensively (Ochi et al., 1999; Zitha et al., 2013). The phenomenon of particle deep bed filtration followed by the formation of external filter cake is not described in the above classical DBF models (Tien, 2012).

Moreover, the oversimplified DBF model using the overall particle concentrations does not account for the effect of pore and particle size distributions on permeability decline in field cases (Veerapen et al., 2001; Massei et al., 2002; Windarto et al., 2012). Glenn and Slusser (1957) reported that certain distribution of particle sizes may reduce the permeability impairment for a given pore size distribution, i.e., the particle size distribution must be accounted for in the cake formation model. Corapcioglu and Abboud (1990) developed a model for cake filtration process accounting for different size particle penetration at the cake surface and migration in the cake. Furthermore, the compressibility effect of the external cake is taken into account with the modelling of the cake growth dynamics considering cake filtration (Sherwood and Meeten, 1997; Tien et al., 1997; Lohne et al., 2010). Civan (1998a, 1998b) investigated cake formation and stabilisation for cross flow filtration. The kinetics model accounts for erosion rate, which is proportional to the difference between the critical and current values of the shear stress. Non-Newtonian fluid properties are taken into account. The analytical models have been derived. Good agreement between the modelling and experimental data has been observed for both linear and radial flows.

The traditional model presents a linear growth of pressure drop over time along the core and its abrupt increase during the external filter cake formation. It results in the delay of external cake formation if compared to particle penetration into the rock. The growth of internal cake formed by the fine particles inside the external cake after the transition time is not accounted for in the models for either drilling fluid invasion or water injectivity (Pang and Sharma, 1997; Wennberg and Sharma, 1997; Suri and Sharma, 2004; Bedrikovetsky et al., 2005). So, the above models assume DBF occurring before the transition time and build-up of external cake afterwards. Yet, in practice, a significant fraction of particles in drilling fluid exceeds pore sizes, so the formation of external cake starts at the beginning of injection, simultaneously with fine particle DBF (Abrams, 1977; Hands et al., 1998; Massei et al., 2002; Tien, 2012).

To the best of our knowledge, the mathematical model for cake filtration that accounts for co-occurring deep bed filtration and cake formation as well as internal cake formed by small particles inside the external cake by large particles is not available in the literature.

The present work aims to partly fill the gap considering injection of bi-sized suspension in the rock. The large particles start building the cake at the beginning of injection; while the small particles simultaneously filtrate through the built-up cake and penetrate into the porous media. After the transition time, the small particles filtrate in the external cake only. The aim of the present work is to develop a mathematical model for cake filtration (i.e. cake formation and deep bed filtration), including the external cake formation by large particles, DBF of small particles, internal cake growth inside external cake after the transition time, and possible formation of mixture cake after the catching-up time. Besides, the laboratory experiments on the injection of bi-sized suspension into a reservoir core have been performed. The results obtained from the proposed model match the laboratory data with high accuracy, which validates the model proposed.

The structure of the paper is as follows. First, the traditional deep bed filtration and cake formation model for mono-size particles is briefly reviewed. It is followed by the development of advanced two-size particle model for external cake formation. Afterwards, the obtained results applying the proposed model are analysed. Finally, the treatment of data from laboratory tests validates the present model.

2. Traditional deep bed filtration and cake formation model for mono-size particles

In this section, the traditional model describing external cake formation and deep bed filtration of mono-size particles in porous media is reviewed. The assumptions of the model include cake formed by compact particle packing, constant porosity of the core and the cake due to low retention of particles, and incompressibility of particle suspension and cake.

Traditional theory considers mono-modal narrow particle size distribution and focused mostly on two extremes: (a) particles larger than pores and (b) particles much smaller than pores.

Let us start from the simplest case, in which the injected particle size is larger than all the pore sizes in the media. Therefore, particles accumulate outside the core inlet and form the external cake. There is no deep bed filtration in this case. Darcy's equation

$$\frac{\partial P}{\partial x} = -\frac{\mu U}{k} \tag{1}$$

is integrated in terms of the distance x to calculate the pressure drop in the core

$$\Delta P_m = \frac{\mu U L}{k_m} \tag{2}$$

and the pressure drop in the cake

$$\Delta P_{ec} = \frac{\mu U L_c(t)}{k_{ec}} \tag{3}$$

The total pressure drop is the sum of these two parts

$$\Delta P = \Delta P_m + \Delta P_{ec} = \mu U\left[\frac{L}{k_m} + \frac{L_c(t)}{k_{ec}}\right] \tag{4}$$

where k_m and k_{ec} are the permeability of the core and cake, respectively; L and $L_c(t)$ stand for the length of the core and thickness of external cake, respectively. μ is the viscosity of injected suspension and U is the Darcy velocity. The total pressure drop ΔP is a linear function of time.

In the case of injected particle size smaller than the pore size of the media, particles first filtrate into porous media, then followed by the formation of external cake after a certain moment (transition time). The model describing this process consists of the following two equations:

Population balance of total suspended and retained particles

$$\frac{\partial}{\partial t}(\phi c + \sigma) + U\frac{\partial c}{\partial x} = 0 \tag{5}$$

Kinetics equation of particle retention

$$\frac{\partial \sigma}{\partial t} = \lambda c U \tag{6}$$

as well as the initial and boundary conditions $t=0$: $c(x,0)=\sigma(x,0)=0$; $x=0$: $c(0,t)=c^0$. The filtration coefficient is denoted as λ.

The retained particle concentration $\sigma(x,t)$ is solved from Eqs. (5) and (6) and applied to the formula for pressure drop along the core

$$\Delta P_m = \mu U \int_0^L \frac{1+\beta\sigma(x,t)}{k_m(0)}\,dx \tag{7}$$

in which β is the formation damage coefficient. The pressure drop in the external cake is calculated using Eq. (3). The sum of these two parts gives the total pressure drop

$$\Delta P = \Delta P_m + \Delta P_{ec} = \mu U\left[\int_0^L \frac{1+\beta\sigma(x,t)}{k_m(0)}dx + \frac{L_c(t)}{k_{ec}}\right] \tag{8}$$

3. Deep bed and external filtration of two-size particles

In this section, the model of external cake formation with injection of two-size particle is derived.

The size of injected small particles r_s is smaller than pore size r_p, while the size of injected large particles r_l is larger than r_p (Fig. 1). The process of small particle deep bed filtration in the core and simultaneous external cake formation described by the present model can be divided into three stages as follows (Fig. 2):

In Stage 1 (Fig. 2a,b), large particles cannot enter the porous medium and only form the external cake from the beginning of injection, since $r_1 > r_p$. Small particles filtrate through the cake and into the core ($r_s < r_p$). Suspended particle concentration in the core decreases, while the retention concentration increases. At the transition moment, the retained particle concentration reaches its critical value at the core inlet. No particles can enter the core after the transition moment. This is the end of Stage 1.

The total pressure drop $\Delta P = \Delta P_{ec} + \Delta P_m$, where ΔP_{ec} and ΔP_m represent the pressure drops in the external cake and in the porous medium, respectively:

$$\begin{aligned}\Delta P_{ec} = {} & \frac{\mu U L}{k_{ec}(0)}\left[D_1 + \beta\phi_3 c_3^0 (D_1+1)\right]T \\ & + \frac{\mu U L}{k_{ec}(0)}\beta\phi_3 c_3^0 \frac{(D_1+1)^2}{D_1\lambda_c}\left[\exp\left(-\lambda_c\frac{D_1 T}{(D_1+1)}\right) - 1\right]\end{aligned} \tag{9}$$

$$\begin{aligned}\Delta P_m = {} & \frac{\mu U L}{k_m(0)}\left\{1 + \beta\phi_1 C_3^0 \lambda \frac{D_1+1}{\lambda_c D_1}\left[\frac{1}{\lambda}(1-\exp(-\lambda)) \right.\right. \\ & - \frac{R(D_1+1)}{\lambda_c D_1 - R\lambda(D_1+1)}\left(\exp\left(\frac{\lambda_c D_1 - R\lambda(D_1+1)}{R(D_1+1)} - \frac{\lambda_c D_1 T}{D_1+1}\right)\right. \\ & \left.\left.\left. - \exp\left(-\frac{\lambda_c D_1 T}{D_1+1}\right)\right)\right]\right\}\end{aligned} \tag{10}$$

The derivation of pressure drops (9) and (10) is provided in the Appendix B.

In Stage 2 (Fig. 2c), the external cake formed by large particles keeps growing. Small particles start to accumulate outside the core inlet and form the internal cake inside the external cake of large particles. The retained particle concentration in the core is unchanged, since no more particles can penetrate into the medium.

The total pressure drop $\Delta P = \Delta P_m + \Delta P_{ec1} + \Delta P_{ec2}$, in which the three components ΔP_m, ΔP_{ec1} and ΔP_{ec2} are the pressure drop in the medium, between the fronts of external and internal cakes,

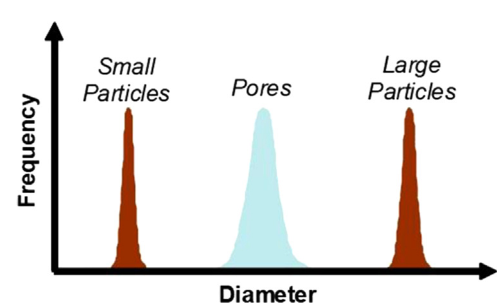

Fig. 1. Large particles do not penetrate into the media and start forming the cake at once while small particles perform deep bed filtration in the media.

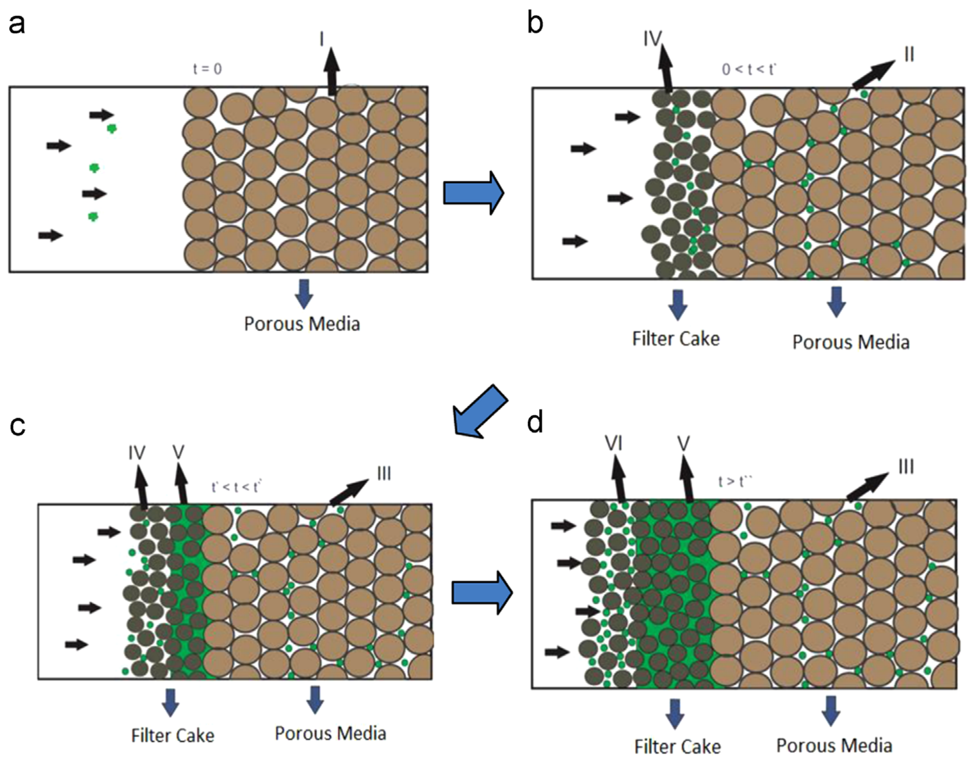

Fig. 2. Two scenarios for two-size particle cake formation: (a) beginning of two-size particle suspension injection; (b) deep bed filtration of small particles with simultaneous formation of cake by large particles; (c) small particles start filling pore space of the cake after the transition time; (d) development of the mixed-particle cake after small particle cake front catching up with the large particle cake front. Zone I: clean core at $t=0$; Zone II: DBF of small particles in the core; Zone III: unchanged retention concentration profile in the core; Zone IV: small particles filtration in external cake; Zone V: internal cake growth inside external cake; Zone VI: new cake formed by mixed two-size particles.

and between the front of internal cake and core inlet, respectively:

$$\Delta P_m = \frac{\mu UL}{k_m(0)}\left\{1+\beta\phi_1 C_3^0\lambda\frac{D_1+1}{\lambda_c D_1}\left[\frac{1}{\lambda}(1-\exp(-\lambda)) - \frac{R(D_1+1)}{\lambda_c D_1 - R\lambda(D_1+1)}\left(\exp\left(\frac{\lambda_c D_1 - R\lambda(D_1+1)}{R(D_1+1)} - \frac{\lambda_c D_1 T_{tr}}{D_1+1}\right) - \exp\left(-\frac{\lambda_c D_1 T_{tr}}{D_1+1}\right)\right)\right]\right\} \quad (11)$$

$$\Delta P_{ec1} = \frac{\mu UL}{k_{ec}(0)}\left[1+\beta\phi_3 c_3^0\frac{(D_1+1)}{D_1}\right](D_1 T + z(T)) + \frac{\mu UL}{k_{ec}(0)}\beta\phi_3 c_3^0\frac{(D_1+1)^2}{D_1\lambda_c}\left[\exp\left(-\lambda_c\frac{D_1 T + z(T)}{(D_1+1)}\right)-1\right] \quad (12)$$

$$\Delta P_{ec2} = \frac{\mu UL}{k_{ec12}}(-z(T)) \quad (13)$$

in which the thickness of internal cake $z(T)$ is calculated from

$$z(T) = \frac{D_1+1}{\lambda_c}\ln\left[\left(1-\frac{c_3^0\exp(-((\lambda_c D_1)/(D_1+1))T_{tr})}{(1-\phi_2)D_1}\right)\exp\left(\frac{\lambda_c D_1}{D_1+1}T\right) + \frac{c_3^0}{(1-\phi_2)D_1}\right] - D_1 T \quad (14)$$

Derivations of Eqs. (11)–(14) are given in the Appendix C.

The front moving speed of the external cake formed by large particles may differ from that of the internal cake formed by small particles. It depends on the concentration ratio of small and large particles in the injected suspension as well as the porosities of the core and the cake. If the internal cake front moves slower than the front of the external cake, Stage 2 continues. Otherwise, if the front of internal cake moves faster than that of the external cake, the internal cake front catches up with the external cake front. Stage 2 transits to Stage 3 at the catching-up time.

In Stage 3 (Fig. 2d), a new cake formed by the mixture of two-size particles begins to grow. The total pressure drop in this stage $\Delta P = \Delta P_m + \Delta P_{ec} + \Delta P_{ecmix}$, where the three components ΔP_m, ΔP_{ec} and ΔP_{ecmix} are the pressure drop in the medium, from the intersection of the two cake fronts to the core inlet, and in the mixture cake, respectively:

$$\Delta P_{ec} = -\frac{\mu UL}{k_{ec12}}D_1 T_3 \quad (15)$$

$$\Delta P_{ecmix} = \frac{\mu UL}{k_{ecmix}}D_3(T-T_3) \quad (16)$$

and ΔP_m is calculated by Eq. (11). The catching-up time T_3 is obtained from

$$T_3 = \frac{D_1+1}{\lambda_c D_1}\ln\left[\frac{1-c_3^0/((1-\phi_2)D_1)}{1-c_3^0\exp(-((\lambda_c D_1)/(D_1+1)))T_{tr}/((1-\phi_2)D_1)}\right] \quad (17)$$

Eqs. (15)–(17) are derived in the Appendix D.

For constant injection rate, the impedance caused by cake formation is the ratio of total pressure drop at time T and the initial pressure drop

$$J = \frac{\Delta P(T)}{\Delta P(0)} \quad (18)$$

The complete set of formulae for impedance profile in all stages is summarised in Table 1.

Table 1
Formulae for impedance profile at each stage.

Time interval	Impedance (*J*)
$T<T_{tr}$	$J_{ec}=\frac{1}{\Delta p_0}\left\{\frac{\mu UL}{k_{ec}(0)}[D_1+\beta\phi_3 c_3^0(D_1+1)]T+\frac{\mu UL}{k_{ec}(0)}\beta\phi_3 c_3^0\frac{(D_1+1)^2}{D_1\lambda_c}\left[\exp\left(-\lambda_c\frac{D_1T}{(D_1+1)}\right)-1\right]\right\}$
	$J_m=\frac{1}{\Delta p_0}\left\{\frac{\mu UL}{k_m(0)}\left\{1+\beta\phi_1 C_3^0\lambda\frac{D_1+1}{\lambda_c D_1}\left[\frac{1}{\lambda}(1-\exp(-\lambda))-\frac{R(D_1+1)}{\lambda_c D_1-R\lambda(D_1+1)}\left(\exp\left(\frac{\lambda_c D_1-R\lambda(D_1+1)}{R(D_1+1)}-\frac{\lambda_c D_1 T}{D_1+1}\right)-\left(\exp-\frac{\lambda_c D_1 T}{D_1+1}\right)\right)\right]\right\}\right\}$
	$J=J_{ec}+J_m$
$T_{tr}<T<T_3$	$J_{ec1}=\frac{1}{\Delta p_0}\left\{\frac{\mu UL}{k_{ec}(0)}\left[1+\beta\phi_3 c_3^0\frac{(D_1+1)}{D_1}\right](D_1T+z(T))+\frac{\mu UL}{k_{ec}(0)}\beta\phi_3 c_3^0\frac{(D_1+1)^2}{D_1\lambda_c}\left[\exp\left(-\lambda_c\frac{D_1T+z(T)}{(D_1+1)}\right)-1\right]\right\}$
	$J_{ec2}=\frac{1}{\Delta p_0}\frac{\mu UL}{k_{ec12}}(-z(T))$
	where $z(T)=\frac{D_1+1}{\lambda_c}\ln\left[\left(1-\frac{c_3^0\exp(-\frac{\lambda_c D_1}{D_1+1}T_{tr})}{(1-\phi_2)D_1}\right)\exp\left(\frac{\lambda_c D_1}{D_1+1}T\right)+\frac{c_3^0}{(1-\phi_2)D_1}\right]-D_1T$
	$J_m(T_{tr})=\frac{1}{\Delta p_0}\frac{\mu UL}{k_m(0)}\left\{1+\beta\phi_1 C_3^0\lambda\frac{D_1+1}{\lambda_c D_1}\left[\frac{1}{\lambda}(1-\exp(-\lambda))-\frac{R(D_1+1)}{\lambda_c D_1-R\lambda(D_1+1)}\left(\exp(\frac{\lambda_c D_1-R\lambda(D_1+1)}{R(D_1+1)}-\frac{\lambda_c D_1 T_{tr}}{D_1+1})-\exp(-\frac{\lambda_c D_1 T_{tr}}{D_1+1})\right)\right]\right\}$
	$J=J_{ec1}+J_{ec2}+J_m(T_{tr})$
$T<T_3$	$J_{ec}=-\frac{1}{\Delta p_0}\frac{\mu UL}{k_{ec12}}D_1T_3$
	$J_{ecmix}=\frac{1}{\Delta p_0}\frac{\mu UL}{k_{ecmix}}D_3(T-T_3)$
	$J_m(T_{tr})=\frac{1}{\Delta p_0}\frac{\mu UL}{k_m(0)}\left\{1+\beta\phi_1 C_3^0\lambda\frac{D_1+1}{\lambda_c D_1}\left[\frac{1}{\lambda}(1-\exp(-\lambda))-\frac{R(D_1+1)}{\lambda_c D_1-R\lambda(D_1+1)}\left(\exp\left(\frac{\lambda_c D_1-R\lambda(D_1+1)}{R(D_1+1)}-\frac{\lambda_c D_1 T_{tr}}{D_1+1}\right)-\exp\left(-\frac{\lambda_c D_1 T_{tr}}{D_1+1}\right)\right)\right]\right\}$
	$J=J_m+J_{ec}+J_{ecmix}$

4. Analysis of modelling results

The results of impedance are calculated from the model developed above for all the three stages. Effects of different parameters on the impedance profile are analysed in this section.

The impedance as a function of time with different injected small particle concentration c_3^0 is shown in Fig. 3. Here the dimensionless time PVI$=$Ut/(ϕ_1L). The larger is c_3^0, the more is the captured particles per unit time, and the earlier is the transition time T_{tr}. The larger is the small particle concentration c_3^0, the faster is the impedance growth at each stage. This is due to the smaller porosity and lower permeability caused by the larger proportion of small particles at each stage. Moreover, the higher fraction of small particles corresponds to the earlier catching-up of the internal cake front.

The impedance curves calculated using different values of internal cake porosity are compared in Fig. 4. If the external cake porosity is fixed, the impedance grows more slowly as the internal cake porosity increases at Stage 2. The value of internal cake porosity does not affect the impedance at other stages. With the constant internal cake porosity in Fig. 5, it is shown that the decrease of external cake porosity leads to faster impedance growth at Stages 1 and 2.

Fig. 6 shows the obtained impedance curves with different values of formation damage coefficient β. A larger formation damage coefficient results in a faster impedance growth at Stage 1. The other two stages are not affected by the value of damage coefficient β in the core.

The impedance as a function of time with different values of medium filtration coefficient λ_m is shown in Fig. 7. Higher value of λ_m indicates a larger number captured particles per unit time, which leads to an earlier transition time. However, the effect of the cake filtration coefficient λ_c on the transition time is negligible (Fig. 8). This is due to the small thickness of the external cake, which results in relatively small number of captured particles in the external cake compared to the injected suspension concentration.

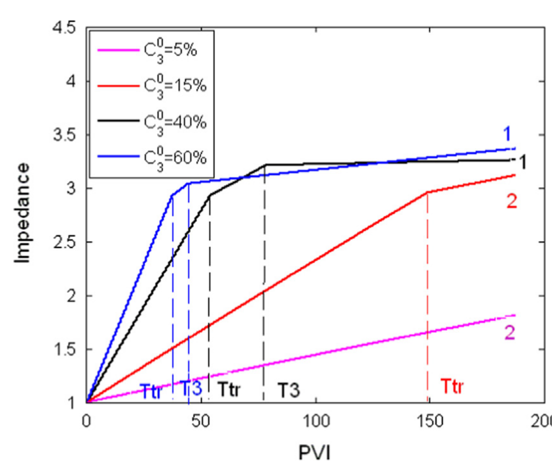

Fig. 3. Impedance curves with different small particle concentrations for two-size model (c_3^0=5%, 15%, 40%, 60%). Scenario 1: internal cake front can catch up with the external cake front; Scenario 2: internal cake front cannot catch up with the external cake front. T_{tr} is the transition time. T_3 is the catching-up time in the first scenario.

Fig. 9 delivers the impedance curves obtained using different value of the critical coefficient $\alpha=\sigma(0,T_{tr})/\phi$. The smaller is the

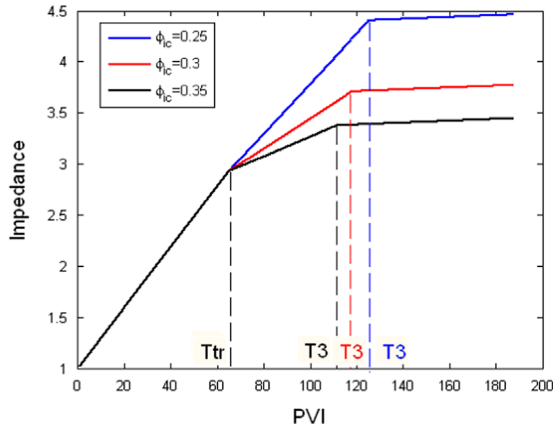

Fig. 4. Impedance curves with different internal cake porosity ϕ_{ic}.

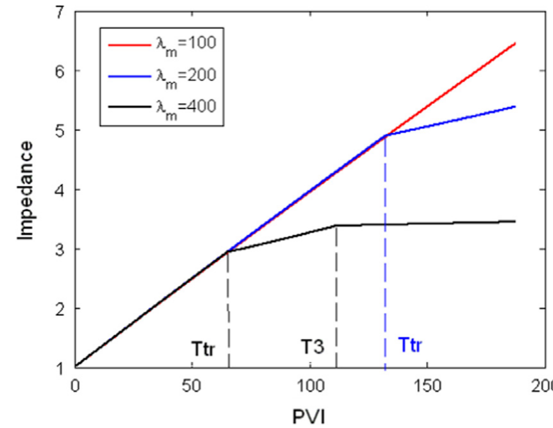

Fig. 7. Impedance curves for different formation filtration coefficients λ_m.

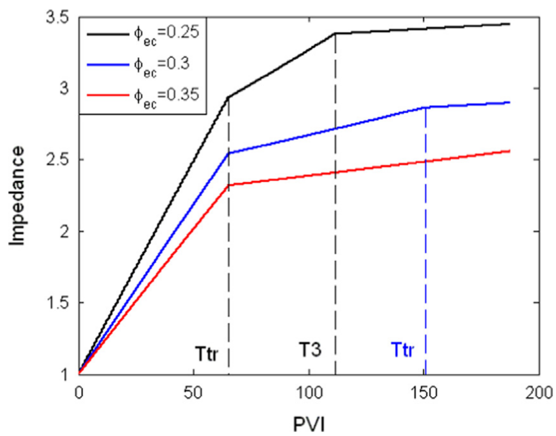

Fig. 5. Impedance curves with different external cake porosity ϕ_{ec}.

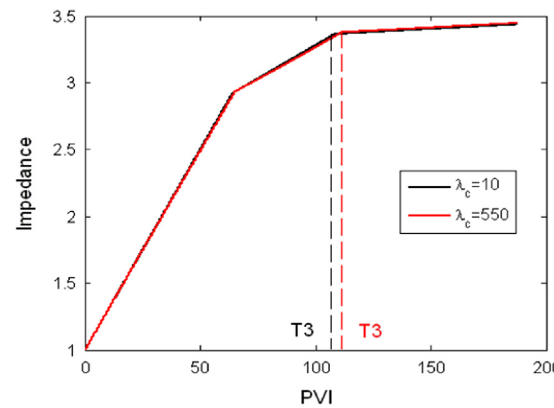

Fig. 8. Impedance curve behaviour for different cake filtration coefficients λ_c.

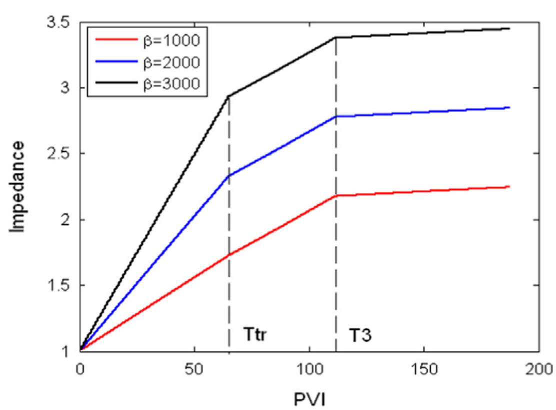

Fig. 6. Impedance versus time for different values of formation damage coefficient β.

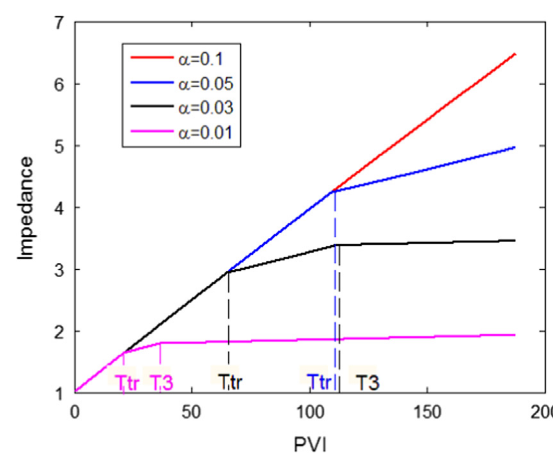

Fig. 9. Impedance curves for different critical porosity coefficients α.

critical coefficient, the earlier is the transition time. Furthermore, the catching-up time of the internal cake front T_3 reduces with α due to the smaller thickness of external cake at the transition time.

5. Experimental validation

Laboratory test on the process of particle deep bed filtration and external cake formation has been performed using the Berea Sandstone core. In the experiment, the injected large and small particle concentrations are 50 and 25 ppm, respectively. The diameters of large and small particles are 100 and 1 μm, respectively. The core length is 4.7 cm, core permeability is 317 md and porosity is 0.2. The diameter of the core cross-section is 3.8 cm.

The impedance profile calculated from the measured data is treated by the two-size model accounting for two scenarios (Fig. 10). The tuning parameters for Scenario 1 are as follows: the critical coefficient $\alpha=0.03$, formation damage coefficient $\beta=3200$, external cake porosity $\phi_1=0.24$, porosity of internal cake $\phi_2=0.35$. The tuning parameters for Scenario 2 are: $\alpha=0.03$, formation damage coefficient $\beta=4500$, external cake porosity $\phi_1=0.38$, porosity of internal cake $\phi_2=0.20$. The permeabilities of external and internal cakes are calculated from the Kozney–Carman formula (A-8).

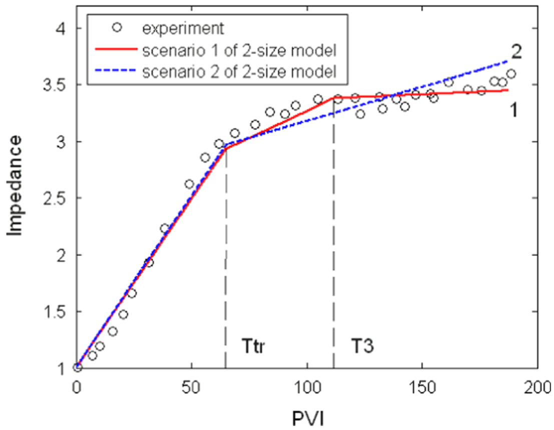

Fig. 10. Impedance profile prediction accounting for different scenarios of the two-size model. Scenario 1: internal cake front can catch up with the external cake front; Scenario 2: internal cake front cannot catch up with the external cake front. T_{tr} is the transition time. T_3 is the catching-up time in the first scenario. (For interpretation of the references to colour in this figure, the reader is referred to the web version of this article.)

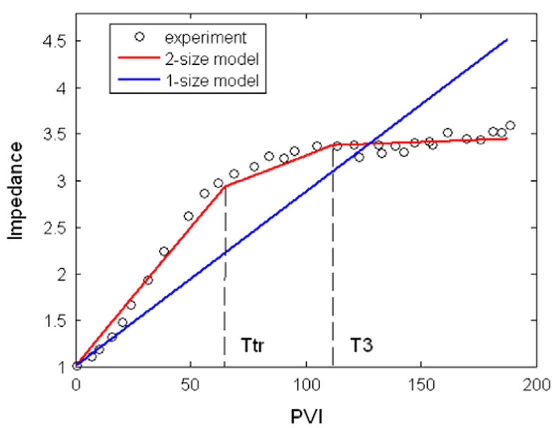

Fig. 11. Comparison of impedance profile using the present two-size model and the traditional mono-size model. T_{tr} is the transition time. T_3 is the catching-up time in the two-size model.

In Scenario 1, the internal cake front can catch up with the external cake front. Therefore, all the three stages exist (see the red curve in Fig. 10). Scenario 2 corresponds to the case that internal cake front cannot catch up with the external cake front. Only Stages 1 and 2 appear in this scenario (the blue dashed curve in Fig. 10). It is clear that the first scenario results in a better agreement between the experimental data and the model prediction than the second scenario.

Comparison of the impedance prediction between the proposed two-size model and the traditional mono-size model is presented in Fig. 11. It is worth noting that the averaged particle size applied in the mono-size model is larger than the pore sizes, therefore all the particles accumulate to form the external cake and no DBF happens in the core. There is no transition time in the mono-size model, which causes the predicted curve using the traditional model deviates from the measured impedance profile (the coefficient of determination $R^2=0.620$). The present two-size model predicts the transition time and the catching-up time successfully and agree well with the impedance profile from lab data ($R^2=0.985$).

So, the mathematical model for deep bed filtration and external cake formation during the injection of bi-sized suspension exhibit more complex behaviour than the mono-sized model. Moreover, the mono-sized model cannot match the laboratory data on bi-sized suspension injection, while the bi-sized suspension injection model matches the laboratory data with high accuracy. It allows expecting that the developed bi-sized suspension injection model can match well with the data on injection of water with particles or invasion of drilling fluids and, therefore, can be used in the design and planning of these processes. However, additional studies are required to support this claim.

6. Conclusions

Mathematical modelling and laboratory experiments on the injection of two-size particle suspension in porous media allow drawing the following conclusions:

The external filter cake formation during injection of two-size particle suspension in porous media can be described by the analytical model. Pressure drop along the core and cake, as well as the suspended and retained particle concentrations can be expressed by explicit formulae.

Two different regimes of cake formation have been distinguished in the model and in laboratory experiments: (1) slow growth of the external large-particle cake with fast moving of the small-particle cake front inside the large-particle cake followed by further cake build-up from the mixture of injected particles; (2) fast growth of the external large-particle cake with slow development of the internal small-particle cake filled in the large-particle cake.

The first regime is typical for high concentration of small particles in the injected suspension, which exhibits piecewise impedance curve with three segments; while the second regime takes place for low concentration of small particles, presenting two-segment piecewise impedance curve.

Treatment of the laboratory test data by the analytical model shows that the first regime of the external cake formation has been occurring in the experiment.

The experimental data on two-size particle injection with deep bed filtration and external cake formation can be matched by the analytical model with high accuracy. Good agreement between the laboratory and modelling data validates the proposed two-size model, which delivers better prediction of the impedance profile than the traditional mono-size particle cake model.

Mathematical modelling using the analytical solution shows that the larger is the injected concentration of small particle, the faster is the impedance growth at each stage. It is explained by smaller porosity and permeability resulting from small particles.

Acknowledgements

Financial support from the Australian Research Council (ARC) Discovery Project 1094299, Linkage Projects 100100613 and 110200799 is gratefully acknowledged.

Appendix A. Governing equations and analytical solution for particle deep bed filtration

Consider injection of suspension with two-size particles. Particles with the larger size are larger than all the pore throats. Hence, they cannot enter the porous medium; instead, they form the external filter cake from the beginning of injection. Small particles injected first filtrate through the external cake formed by large particles and then penetrate in the porous rock.

System of equations for particle deep bed filtration consists of the population balance equation for all the small particles

$$\frac{\partial}{\partial t}(\phi c+\sigma)+U\frac{\partial c}{\partial x}=0 \tag{A-1}$$

and the kinetics equation of particle capture

$$\frac{\partial \sigma}{\partial t}=\lambda cU \tag{A-2}$$

Darcy's law is applied to calculate the pressure drop along the distance

$$U=-\frac{k}{\mu(1+\beta\sigma)}\frac{\partial p}{\partial x} \tag{A-3}$$

Introduction of dimensionless variables and parameters

$$X\rightarrow\frac{x}{L},\quad T\rightarrow\frac{Ut}{\phi L},\quad C=\frac{c}{c_3^0},\quad S=\frac{\sigma}{\phi c_3^0},\quad \lambda=\lambda_0 L,\quad P=\frac{k}{U\mu L}p \tag{A-4}$$

into Eqs. (A-1)–(A-3) yields the following dimensionless system of governing equations

$$\frac{\partial(C+S)}{\partial T}+\frac{\partial C}{\partial X}=0 \tag{A-5}$$

$$\frac{\partial S}{\partial T}=\lambda C \tag{A-6}$$

$$1=-\frac{1}{1+\phi c_3^0\beta S(X,T)}\frac{\partial P}{\partial X} \tag{A-7}$$

Here μ is the viscosity of suspension, U is the Darcy velocity, β is the formation damage coefficient, λ is the dimensionless filtration coefficient, which is denoted as λ_c for the filter cake and λ_m for the porous medium. c_3^0 is the injected small particle concentration, and C is the dimensionless particle concentration. σ is the retained particle concentration, and S is the dimensionless retained particle concentration. L is the core length, ϕ is the porosity. For convenience, ϕ_1 and ϕ_3 are introduced in the model for porous media porosity and external cake porosity, respectively. $k(0)$ is the initial permeability, $k_m(0)$ and $k_{ec}(0)$ stand for the initial permeability of the porous medium and that of the external cake, respectively.

The initial permeability is calculated using the Kozney–Carman equation (Civan, 2007)

$$k(0)=\frac{1}{72\tau}\frac{\phi^3 D_p^2}{(1-\phi)^2} \tag{A-8}$$

here τ is the tortuosity and D_p is the particle diameter.

The analytical model presented below is based on the solution of the initial-boundary problem for constant concentration suspension injection into a clean bed. The initial and boundary conditions are

$$t=0:\ C=S=0$$

$$x=0:\ C=1 \tag{A-9}$$

The solution to the equation system (A-5)–(A-7) with conditions (A-9) is obtained as

$$C(X,T)=\begin{cases} e^{-\lambda X}, & X<T \\ 0, & X>T \end{cases} \tag{A-10}$$

$$S(X,T)=\begin{cases} \lambda(T-X)e^{-\lambda X}, & X<T \\ 0, & X>T \end{cases} \tag{A-11}$$

Appendix B. Pressure drop in the first stage of cake formation (before transition time): $0<T<T_{tr}$

The characteristic curve passing through a point (X, T) crosses the external cake front at the point ($-D_1T_2$, T_2), so

$$D_1T_2+X=T-T_2,\quad T_2=\frac{T-X}{D_1+1} \tag{B-1}$$

where D_1 corresponds to the speed of external filter cake built of the large particles. It is obtained from the mass conservation of injected large particles: $D_1=\phi_3 c_2^0/(1-\phi_3)$.

Substituting Eq. (B-1) into (A-10) results in the suspended particle concentration in external cake

$$C(X,T)=\exp\left[-\lambda_c(D_1T_2+X)\right]=\exp\left[-\lambda_c\frac{D_1T+X}{D_1+1}\right] \tag{B-2}$$

Retained concentration of particles $S(X, T)$ is derived by integration of (B-2) in terms of T from $-X/D_1$ to T

$$S(X,T)=\frac{D_1+1}{D_1}\left\{1-\exp\left[-\lambda_c\frac{D_1T+X}{D_1+1}\right]\right\} \tag{B-3}$$

Finally, the pressure drop over the external cake is obtained by using the Darcy's law

$$\Delta p_{ec}=\frac{\mu UL}{k_{ec}(0)}\int_{-D_1T}^{0}(1+\beta\phi_3 c_3^0 S(X,T))dX \tag{B-4}$$

which is expressed as

$$\Delta p_{ec}=\frac{\mu UL}{k_{ec}(0)}[D_1+\beta\phi_3 c_3^0(D_1+1)]T + \frac{\mu UL}{k_{ec}(0)}\beta\phi_3 c_3^0\frac{(D_1+1)^2}{D_1\lambda_c}\left[\exp\left(-\lambda_c\frac{D_1T}{(D_1+1)}\right)-1\right] \tag{B-5}$$

At the core inlet, the suspended concentration, as it follows from (B-2), is

$$X=0:\ C(0,T)=\exp\left[-\lambda_c\frac{D_1T}{D_1+1}\right] \tag{B-6}$$

The propagation velocities are different in the cake and in the core. The coefficient $R=\phi_3/\phi_1$ is used to normalise the propagation velocity in the core based on that in the external cake

$$\frac{dX}{dT}=R=\frac{\phi_3}{\phi_1} \tag{B-7}$$

The characteristic curve crossing the point (X, T) intersects the core inlet at the moment T'. Integrating the above Eq. (B-7) leads to

$$\int_0^X dX=R\int_{T'}^{T}dT \tag{B-8}$$

Thus, we have

$$T'=T-\frac{1}{R}X \tag{B-9}$$

The characteristic curve covers the distance D_1T_1 inside the external cake and distance x in the core. We can calculate the particle concentration by the new boundary condition $x=0:\ C=C(0,T)$

$$C(X,T)=\exp(-\lambda_c D_1T_1)\exp(-\lambda X)=\exp\left(-\lambda_c D_1\frac{T'}{D_1+1}\right)\exp(-\lambda X)=\exp\left(-\lambda_c D_1\frac{T-X/R}{D_1+1}\right)\exp(-\lambda X) \tag{B-10}$$

Retained concentration $S(X, T)$ is found by integrating the above equation in terms of t from X/R to T

$$S(X,T)=\lambda\exp(-\lambda X)\frac{D_1+1}{\lambda_c D_1}\left[1-\exp\left(-\lambda_c D_1\frac{T-X/R}{D_1+1}\right)\right] \tag{B-11}$$

From (B-11), we have

$$S(0,T)=\lambda\frac{D_1+1}{\lambda_c D_1}\left[1-\exp\left(-\lambda_c D_1\frac{T}{D_1+1}\right)\right] \qquad (B-12)$$

It allows calculating the transient time T_{tr}

$$\frac{\phi_1\alpha}{c_3^0\phi_3}=\lambda\frac{D_1+1}{\lambda_c D_1}\left\{1-\exp\left[-\lambda_c\frac{D_1T_{tr}}{D_1+1}\right]\right\} \qquad (B-13)$$

which results in

$$T_{tr}=-\frac{D_1+1}{\lambda_c D_1}\ln\left(1-\frac{(\phi_1/\phi_3)\alpha\lambda_c D_1}{c_3^0(D_1+1)\lambda}\right) \qquad (B-14)$$

The pressure drop in porous medium is obtained by using the Darcy's law

$$\Delta p_m=\frac{\mu UL}{k_m(0)}\int_0^1(1+\beta\phi_1 c_3^0 S(X,T))dX \qquad (B-15)$$

Substituting Eq. (B-11) into the above Eq. (B-15), we have ΔP_m as

$$\Delta p_m=\frac{\mu UL}{k_m(0)}\left\{1+\beta\phi_1 c_3^0\lambda\frac{D_1+1}{\lambda_c D_1}\left[\frac{1}{\lambda}(1-\exp(-\lambda)) -\frac{R(D_1+1)}{\lambda_c D_1-R\lambda(D_1+1)}\left(\exp\left(\frac{\lambda_c D_1-R\lambda(D_1+1)}{R(D_1+1)}-\frac{\lambda_c D_1 T}{D_1+1}\right) -\exp\left(-\frac{\lambda_c D_1 T}{D_1+1}\right)\right)\right]\right\} \qquad (B-16)$$

Thus, the total pressure drop is obtained by the sum of the pressure drop over the external cake and that in the porous medium.

Appendix C. Pressure drop in the second stage of cake formation (interval between transition time and cake front catching-up time): $T_{tr}<T<T_3$

After the transition time T_{tr}, small particles cannot penetrate into the core anymore. Therefore, suspension concentration at the core inlet is zero, and retained particle concentration remains constant.

At the moment T_{tr}, the internal cake formed by injected small particles starts to accumulate inside the external cake of large particles; simultaneously, injected small particles still filtrate in the external cake and can be captured before reaching the front of the internal cake.

Suspension concentration at the front of internal cake, which propagates inside the external cake $X=z(T)$, as it follows from (B-2), is given by

$$C(z(T),T)=\exp\left[-\lambda_c\frac{D_1T+z(T)}{D_1+1}\right] \qquad (C-1)$$

The moving speed of the internal cake front is obtained from the mass balance of injected small particles:

$$\frac{dz}{dT}=\frac{C(z,T)c_3^0}{1-\phi_2} \qquad (C-2)$$

where ϕ_2 is the porosity of the internal cake formed by the small particles. Combining Eqs. (C-1) and (C-2) results in the ordinary differential equation for the internal cake front location $z(T)$

$$\frac{dz}{dT}=\frac{1}{1-\phi_2}\exp\left[-\lambda_c\frac{D_1T+z}{D_1+1}\right] \qquad (C-3)$$

By solving the above equation, we obtain the front location of internal cake $z(T)$ as a function of time T

$$z(T)=\frac{D_1+1}{\lambda_c}\ln\left[\left(1-\frac{c_3^0\exp(-((\lambda_c D_1)/(D_1+1))T_{tr})}{(1-\phi_2)D_1}\right)\exp\left(\frac{\lambda_c D_1}{D_1+1}T\right)+\frac{c_3^0}{(1-\phi_2)D_1}\right]-D_1T \qquad (C-4)$$

The moment when the internal cake front catches up with the front of the external cake T_3 is calculated from the intersection of front trajectories:

$$z(T_3)=-D_1T_3 \qquad (C-5)$$

which leads to the formula for the catching-up time T_3

$$T_3=\frac{D_1+1}{\lambda_c D_1}\ln\left[\frac{1-c_3^0/((1-\phi_2)D_1)}{1-c_3^0\exp(-((\lambda_c D_1)/(D_1+1)))T_{tr}/((1-\phi_2)D_1)}\right] \qquad (C-6)$$

From Eq. (A-7), the pressure drop of the external cake between the fronts of external and internal cake can be derived by integrating in terms of x from $-D_1T$ to $z(T)$

$$\Delta p_{ec1}=\frac{\mu UL}{k_{ec}(0)}\int_{-D_1T}^{z(T)}(1+\beta\phi_3 c_3^0 S(X,T))dX \qquad (C-7)$$

The pressure drop between the front of internal cake and the core inlet can be calculated by the Darcy's law directly

$$\Delta p_{ec2}=-\frac{\mu UL}{k_{ec12}}z(T) \qquad (C-8)$$

where k_{ec12} is the permeability of external cake filled by internal cake of small particles.

Thus, the total pressure drop is the sum of the pressure drop in the porous medium (B-16) at $T=T_{tr}$, that in the external cake between the two cake fronts (C7) and that between the internal cake front and core inlet (C-8), as follows

$$\Delta p=\Delta p_m+\Delta p_{ec1}+\Delta p_{ec2} \qquad (C-9)$$

Appendix D. Pressure drop in the third stage of cake formation (after the cake front catching-up time): $T>T_3$

After the intersection of the fronts of external and internal cakes at point (X_3,T_3), a new cake is formed by the mixture of two size particles (overall injected suspension). The front speed D_3 is obtained from the mass balance of injected large and small particles: $D_3=\phi_3(c_1^0+c_2^0)/(1-\phi_4)$. Here, ϕ_4 is the porosity of the cake formed by two size particles (overall injected suspension). There is no deep bed filtration the third stage.

The pressure drop of the mixture cake formed by two size particles can be obtained from

$$\Delta p_{ecmix}=\frac{\mu UL}{k_{ecmix}}D_3(T-T_3) \qquad (D-1)$$

where k_{ecmix} is the permeability of the mixture cake formed by two size particles.

The pressure drop of the external cake from the intersection of the two cake fronts to the core inlet can be calculated as

$$\Delta p_{ec}=-\frac{\mu UL}{k_{ec12}}D_1T_3 \qquad (D-2)$$

Finally, the total pressure drop can be calculated by

$$\Delta p=\Delta p_m+\Delta p_{ec}+\Delta p_{ecmix} \qquad (D-3)$$

The impedance caused by cake formation for constant injection rate is defined as

$$J=\frac{\Delta p(T)}{\Delta p(0)} \qquad (D-4)$$

References

Abrams, A., 1977. Mud design to minimize rock impairment due to particle invasion. J. Pet. Technol. 29, 586–592.

Bedrikovetsky, P., 2008. Upscaling of stochastic micro model for suspension transport in porous media. Transp. Porous Media 75, 335–369.

Bedrikovetsky, P., et al., 2001. Characterisation of deep bed filtration system from laboratory pressure drop measurements. J. Pet. Sci. Eng. 32 (2–4), 167–177.

Bedrikovetsky, P.G., et al., 2005. Well-history-based prediction of injectivity decline during seawater flooding, SPE European Formation Damage Conference. Society of Petroleum Engineers, Sheveningen, The Netherlands.

Civan, F., 1998a. Incompressive cake filtration: mechanism, parameters, and modeling. AIChE J. 44 (11), 2379–2387.

Civan, F., 1998b. Practical model for compressive cake filtration including fine particle invasion. AIChE J. 44 (11), 2388–2398.

Civan, F., 2007. Reservoir Formation Damage: Fundamentals, Modeling, Assessment, and Mitigation. Gulf Publishing Company, Houston, Texas.

Civan, F., Nguyen, V., 2005. Modeling particle migration and deposition in porous media by parallel pathways with exchange. In: Vafai, K. (Ed.), Handbook of Porous Media, 2nd ed. CRC Press, Boca Raton, FL, pp. 457–484.

Civan, F., Rasmussen, M.L., 2005. Analytical models for porous media impairment by particles in rectilinear and radial flows. In: Vafai, K. (Ed.), Handbook of Porous Media, 2nd ed. CRC Press, Boca Raton, FL, pp. 485–542.

Corapcioglu, M.Y., Abboud, N.M., 1990. Cake filtration with particle penetration at the cake surface. SPE Reserv. Eng. 5 (3), 317–326.

Dalmazzone, C.S., Follotec, A.L., Audibert-Hayet, A., Twynam, A.J., Poitrenaud, H.M., 2007. Development of an Optimized Formulation for Cleaning Water Injection Wells Drilled With Oil-Based Systems, European Formation Damage Conference. Society of Petroleum Engineers, Scheveningen, The Netherlands.

Ding, Y., Herzhaft, B., Renard, G., 2006. Near-wellbore formation damage effects on well performance: a comparison between underbalanced and overbalanced drilling. SPE Prod. Oper. 21 (1), 51–57.

Ding, Y., Longeron, D., Renard, G., Audibert, A., 2004. Modeling of both near-wellbore damage and natural cleanup of horizontal wells drilled with water-based drilling fluids. SPE J. 9 (3), 252–264.

Ding, Y., Renard, G., 2005. Evaluation of horizontal well performance after drilling-induced formation damage. J. Energy Resour. Technol., Trans. ASME 127 (3), 257–263.

Ding, Y., Renard, G., Herzhaft, B., 2008. Quantification of uncertainties for drilling-induced formation damage. SPE Prod. Oper. 23 (2), 221–231.

Ghalambor, A., Economides, M.J., 2002. Formation damage abatement: a quarter-century perspective. SPE J. 7 (1), 4–13.

Glenn, E.E., Slusser, M.L., 1957. Factors affecting well productivity II. Drilling fluid particle invasion into porous media. Pet. Trans. AIME 210, 132–139.

Hands, N., Kowbel, K., Maikranz, S., Nouris, R., 1998. Drill-in fluid reduces formation damage, increases production rates. Oil Gas J. 96 (28), 65–69.

Herzig, J.P., Leclerc, D.M., Legoff, P., 1970. Flow of suspensions through porous media – application to deep filtration. Ind. Eng. Chem. 62 (5), 8–35.

Karimi, M., Ghalambor, A., Montgomery, M., Moellendick, T.E., 2011. Formation Damage and Fluid Loss Reduction due to Plastering Effect of Casing Drilling, SPE European Formation Damage Conference. Society of Petroleum Engineers, Noordwijk, The Netherlands.

Khatib, Z.I., 1994. Prediction of formation damage due to suspended solids: modeling approach of filter cake buildup in injectors, SPE Annual Technical Conference and Exhibition. Society of Petroleum Engineers, New Orleans, Louisiana.

Khilar, K.C., Fogler, H.S., 1998. Migrations of Fines in Porous Media. Theory and Applications of Transport in Porous Media. Kluwer Academic Publishers, Dordrecht, The Netherlands.

Lohne, A., et al., 2010. Formation-damage and well-productivity simulation. SPE J. 15 (3), 751–769.

Massei, N., Lacroix, M., Wang, H.Q., Dupont, J.P., 2002. Transport of particulate material and dissolved tracer in a highly permeable porous medium: Comparison of the transfer parameters. J. Contam. Hydrol. 57 (1–2), 21–39.

Ochi, J., Detienne, J.-L., Rivet, P., 2007. Internal formation damage properties and oil-deposition profile within reservoirs during PWRI operations, European Formation Damage Conference. Society of Petroleum Engineers, Scheveningen, The Netherlands.

Ochi, J., Detienne, J.-L., Rivet, P., Lacourie, Y., 1999. External filter cake properties during injection of produced waters, SPE European Formation Damage Conference. Society of Petroleum Engineers, The Hague, Netherlands.

Ochi, J., Vernoux, J.F., 1999. A two-dimensional network model to simulate permeability decrease under hydrodynamic effect of particle release and capture. Transp. Porous Media 37 (3), 303–325.

Pang, S., Sharma, M.M., 1997. A model for predicting injectivity decline in water-injection wells. SPE Form. Eval. 12 (3), 194–201.

Parn-anurak, S., Engler, T.W., 2005. Modeling of fluid filtration and near-wellbore damage along a horizontal well. J. Pet. Sci. Eng. 46 (3), 149–160.

Payatakes, A.C., Rajagopalan, R., Tien, C., 1974. Application of porous media models to the study of deep bed filtration. Can. J. Chem. Eng. 52, 722–731.

Quintero, L., Jones, T.A., Clark, D., Twynam, A.J., 2007. NAF Filter Cake Removal Using Microemulsion Technology, European Formation Damage Conference. Society of Petroleum Engineers, Scheveningen, The Netherlands.

Ruth, B.F., 1935. Studies in Filtration III. Derivation of General Filtration Equations. Ind. Eng. Chem. 27 (6), 708–723.

Salimi, S., Khansari, A.N., Ghalambor, A., Tronvoll, J., 2009. Application of UBD Technology To Maximize Recovery From Horizontal Wells in the Naturally Fractured Carbonate Reservoirs, IADC/SPE Managed Pressure Drilling and Underbalanced Operations Conference & Exhibition. In: Proceedings of the 2009 IADC/SPE Managed Pressure Drilling and Underbalanced Operations Conference and Exhibition, San Antonio, Texas.

Shapiro, A.A., Bedrikovetsky, P.G., Santos, A., Medvedev, O.O., 2007. A stochastic model for filtration of particulate suspensions with incomplete pore plugging. Transp. Porous Media 67 (1), 135–164.

Sherwood, J.D., Meeten, G.H., 1997. The filtration properties of compressible mud filtercakes. J. Pet. Sci. Eng. 18 (1–2), 73–81.

Suri, A., Sharma, M.M., 2004. Strategies for sizing particles in drilling and completion fluids. SPE J. 9 (1), 13–23.

Tien, C., 2012. Principles of Filtration. Elsevier Science, Boston.

Tien, C., Bai, R., Ramarao, B.V., 1997. Analysis of cake growth in cake filtration: effect of fine particle retention. AIChE J. 43 (1), 33–44.

Veerapen, J.P., Nicot, B., Chauveteau, G.A., 2001. In-depth permeability damage by particle deposition at high flow rates (Copyright 2001). SPE European Formation Damage Conference. , Society of Petroleum Engineers Inc., The Hague, Netherlands.

Wagner, M.R., et al., 2006. Horizontal drilling and openhole gravel packing with oil-based fluids – an industry milestone. SPE Drill. Complet. 21 (1), 32–43.

Wennberg, K.E., Sharma, M.M., 1997. Determination of the filtration coefficient and the transition time for water injection wells (Copyright 1997). SPE European Formation Damage Conference. Society of Petroleum Engineers, Inc., The Hague, Netherlands.

Windarto, W., Gunawan, A.Y., Sukarno, P., Soewono, E., 2011. Modeling of mud filtrate invasion and damage zone formation. J. Pet. Sci. Eng. 77 (3–4), 359–364.

Windarto, Gunawan, A.Y., Sukarno, P., Soewono, E., 2012. Modelling of formation damage due to mud filtrate invasion in a radial flow system. J. Pet. Sci. Eng. 100, 99–105.

You, Z., Badalyan, A., Bedrikovetsky, P., 2013. Size-exclusion colloidal transport in porous media—stochastic modeling and experimental study. SPE J. 18 (4), 620–633.

You, Z., Osipov, Y., Bedrikovetsky, P., Kuzmina, L., 2014. Asymptotic model for deep bed filtration. Chem. Eng. J. 258, 374–385.

Ytrehus, J.D., Cerasi, P., Opedal, N., 2013. Dynamic Fluid Erosion on Filter Cakes, Proceedings of the 10th SPE International Conference and Exhibition on European Formation Damage. Society of Petroleum Engineers, Noordwijk, The Netherlands.

Yuan, H., Shapiro, A.A., 2011. Induced migration of fines during waterflooding in communicating layer-cake reservoirs. J. Pet. Sci. Eng. 78 (3–4), 618–626.

Yuan, H., You, Z., Shapiro, A.A., Bedrikovetsky, P., 2013. Improved population balance model for straining-dominant deep bed filtration using network calculations. Chem. Eng. J. 226, 227–237.

Zitha, P., Frequin, D., Bedrikovetsky, P., 2013. CT Scan Study of the Leak-Off of Oil-Based Drilling Fluids into Saturated Media, Proceedings of the 10th SPE International Conference and Exhibition on European Formation Damage. Society of Petroleum Engineers, Noordwijk, The Netherlands.